



HAL
open science

An Overview of Recent DLR Contributions on Active Flow-Separation Control Studies for High-Lift Configurations

V. Ciobaca, J. Wild

► **To cite this version:**

V. Ciobaca, J. Wild. An Overview of Recent DLR Contributions on Active Flow-Separation Control Studies for High-Lift Configurations. Aerospace Lab, 2013, 6, p. 1-12. hal-01184651

HAL Id: hal-01184651

<https://hal.science/hal-01184651>

Submitted on 17 Aug 2015

HAL is a multi-disciplinary open access archive for the deposit and dissemination of scientific research documents, whether they are published or not. The documents may come from teaching and research institutions in France or abroad, or from public or private research centers.

L'archive ouverte pluridisciplinaire **HAL**, est destinée au dépôt et à la diffusion de documents scientifiques de niveau recherche, publiés ou non, émanant des établissements d'enseignement et de recherche français ou étrangers, des laboratoires publics ou privés.

V. Ciobaca , J. Wild
(DLR)

E-mail: vlad.ciobaca@dlr.de

An Overview of Recent DLR Contributions on Active Flow-Separation Control Studies for High-Lift Configurations

This is an overview of flow control experiments and simulations for flow separation control on high-lift configurations performed over the last seven years at the German Aerospace Center within national and European projects. Emphasis is placed on the low speed atmospheric and cryogenic experimental setups using the DLR F15 high-lift airfoil and on the numerical verification and validation of the Reynolds Averaged Navier Stokes (RANS) solver TAU for active flow control (AFC) simulations. The wind tunnel studies concern leading edge boundary layer control and flap separation control, both by means of pulsed blowing. The computational effort is mostly dedicated to the most promising technology out of the two concepts, namely the pulsed blowing through slots on the trailing edge flap. Experimental examples of successful flow control for enhancement of lift are given for moderate and high Reynolds numbers to prove the feasibility of the technology for implementation on real aircraft. The computational process chain is validated with wind tunnel measurements, but also applied for an optimization of the trailing edge flap shape for separation control.

Introduction

Future transport aircraft can benefit from matured active flow separation control techniques that can support the achievement of a reduced environmental impact of air traffic [1]-[4]. The research results published over the last two decades show the potential of modern flow control for lift increase, drag reduction and dynamic control through problem specific implementation. In addition, the upcoming active technologies, especially the enabling of laminar wing technology, is foreseen to be substantially able to decrease fuel burn by means of aerodynamic enhancements. Therefore, slatless wing configurations with active flow control have become of interest as an alternative to current leading edge devices, like slats or Krueger flaps. By omitting these classical devices, the tracking systems can be suppressed and a benefit in costs and weight is expected. Beyond the complexity improvements, an active control system can support the laminar flow for the upper and lower side of an airfoil, whereas a Krueger for example can typically only assure a laminar flow on the wing suction side, because a backward facing step of small height can be responsible for the transition to turbulent flow on the pressure side and one third of the potential drag reduction is therefore compromised according to recent studies.

On the other hand, slats and Krueger flaps are powerful passive devices for achieving high values of maximum lift [5]. To be applicable, the lift loss resulting from their removal must be recovered. If an increase of approach and landing speed is not meaningful, the lift can only be

recovered by increasing the wing area or enhancing the lift coefficient by means other than a leading edge device. The solutions discussed nowadays are more complex trailing edge devices and active flow separation control.

Today, there are no civil aircraft flying an active flow control system, and this is more than a decade since McLean [3] concluded that modern flow control is the most promising for high-lift applications. The use of active flow control, such as constant or pulsed blowing, suction or zero-mass flux synthetic jet actuation (SJA), or dielectric barrier discharger actuators (DBD), has been since intensively investigated worldwide. The primarily reported drawbacks for implementation on aircraft have been related to the lack of efficient actuation systems, to the structural integrity or, for example, due to too high power demands. Some technologies have reached a specific maturity concerning the aerodynamic discipline. Therefore, an overview of the existing results for specific active technologies is worth discussing.

Over the last seven years, DLR has supported studies of active flow control for high-lift by means of pulsed blowing through inclined holes and slots, with a strong collaboration with universities, namely the Technical University of Berlin (TUB), and the Technical University of Braunschweig (TUBS). Two flow control technologies have shown previously under laboratory conditions to have a high potential for separation control and lift improvement. Tinnap et al. [6] proved the feasibility of flow control through slots with a low Reynolds number

and low-speed flows. Petz et al. [7] investigated the influence of excitation parameters on the efficiency of this flow control method, on a 2D configuration consisting of two NACA airfoils and Becker et al. [8] contributed control strategies to these AFC attempts. Ortmanns and Kähler [9] investigated jet vortex generators placed on a simple flat plate within a detailed parametric study at low speed and low Reynolds numbers. Scholz et al. [10] implemented the most promising of these pneumatic round-jet actuators in the nose region of an airfoil to successfully prevent leading edge separation.

Therefore, DLR has supported experiments for a state-of-the-art supercritical high-lift airfoil, namely DLR-F15, as a platform for combined flow control on the wing leading edge and trailing edge flap. DLR provided access to a large scale experimental test bed that allowed studies at flight relevant inflow speeds and Reynolds numbers, while flow control techniques were implemented by the universities. Summaries of the experimental results will be presented in this article.

Besides the wind tunnel experiment, numerical simulation has become a pillar for the aerodynamics discipline. Numerical simulation is an important method for rapid design and for optimization processes, as well as for the study of scaling effects. Therefore, DLR is keen to make the corresponding numerical simulation methods accessible for the use of modern AFC methods on future transport aircraft. Important progress has been made over the last decade, but numerical tools still require active development for practical solutions of various AFC methods, including validation with high-fidelity experiments. Therefore, the active flow control applications on the DLR F15 airfoil were used for numerical simulations dedicated to the evaluation of flow control capabilities, as well as for direct comparison with the wind tunnel experiment. Basic test cases, such as single-actuator simulations on a zero-pressure gradient flat plate, served as a starting point for the validation of the numerical method [11]. The numerical analysis addressed the constant and the pulsed blowing. Later, the focus was on separation control for the trailing edge flap by the unsteady actuation through slots [12]; [13]. In general, the Computational Fluid Dynamics (CFD) studies discuss the trends for flow control application by parameter variation, such as the blowing frequency, the actuation intensity, or the geometrical actuation direction. Here, the overview includes the specific major findings by CFD and the level of agreement with the experiment. Additionally, it is presented an example of shape optimization for separation control application.

In the following, the flow control experiments carried out at the German Dutch Wind Tunnel (DNW) low speed facilities NWB and KKK are summarized. The DLR F15 tests cover the application of state-of-the-art pulsed blowing actuators for tunnel testing and allow the discussion of the potential to increase lift and control the flow separations at moderate and high Reynolds numbers. Afterwards, numerical steady and unsteady RANS simulations in conjunction with the DLR F15 high-lift airfoil are reported. The computational findings allow the validation with the experiment to be presented and allow the major trends of the various control parameters that can support the later optimization of the energy requirements and/or geometrical parameters to be revealed.

Flow Control High-Lift Experiments

Wind tunnel model DLR-F15

The DLR-F15 wind tunnel model shown in figure 1 is a 2D wall-to-wall high-lift model. The modular main wing allows leading and trailing

edges to be exchanged. Therefore, different types of high-lift elements can be investigated and compared at the same baseline geometry. The clean wing section is derived from a generic high-lift wing investigated in the nationally funded project ProHMS [14] and represents a state-of-the-art transonic turbulent airfoil for a modern civil transport aircraft. The setup of interest for flow control is a 2-element configuration that features a clean leading edge and a single-slotted flap. The device is mounted on continuously adjustable brackets, allowing the free positioning of this element in all three degrees of freedom. The model is equipped with about 220 static pressure taps. One dense pressure distribution is located in the center section and is used for the integration of the aerodynamic coefficients. In addition, two less dense pressure distributions are located close to the tunnel walls, in order to assess the two-dimensionality of the flow. As described in [16], the pressure distribution has been discovered to not be dense enough for an accurate integration of drag coefficients, leading to errors of up to 20%. The pure integration error for lift coefficients is of about 1% and an accuracy of about 3% is achieved for the pitching moment coefficient.

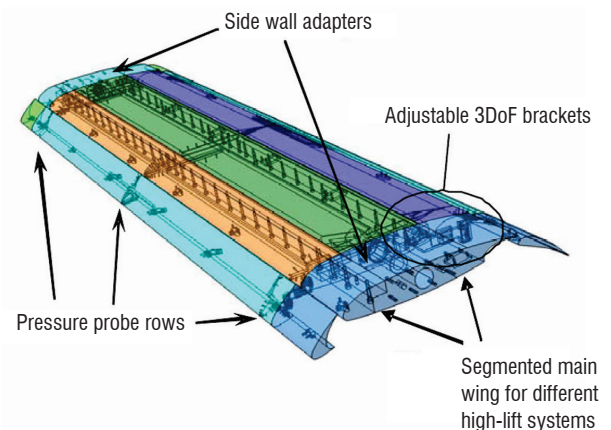
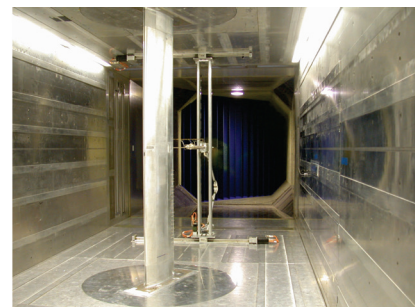
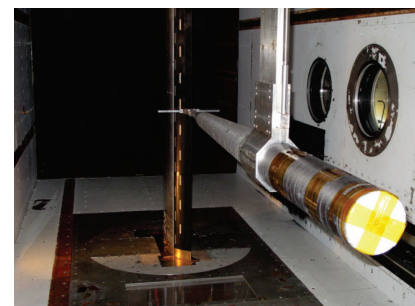


Figure 1 - General arrangement of the DLR F15 two-dimensional high-lift model in 3-element configuration

Wind tunnel test sections



(a) in DNW-NWB, atmospheric tunnel



(b) in DNW-KKK, cryogenic tunnel

Figure 2 - DLR F15 two-dimensional high-lift model mounted in closed test sections of DNW low speed wind tunnels

The reported tests were carried out in the atmospheric wind tunnel DNW-NWB in Braunschweig [15] and in the cryogenic facility DNW-KKK in Cologne (figure 2). These are closed loop low-speed tunnels that operate at approximately ambient pressure. The DNW-NWB facility has a maximum Mach number of $M = 0.27$ and the test section has a cross-section of $3.25 \times 2.8 \text{ m}^2$. In DNW-KKK the temperature can be regulated between ambient and $T = 100\text{K}$; Mach numbers can range between $M = 0.1$ and $M = 0.3$ and the test section has a cross-section of $2.4 \times 2.4 \text{ m}^2$. Based on the aerodynamic clean chord $c = 0.6 \text{ m}$, the maximum Reynolds number achieved was $Re = 3 \times 10^6$ for atmospheric conditions and $Re = 12 \times 10^6$ for the cryogenic testing.

The experimental Mach and Reynolds number dependencies, including the stall behavior of the baseline airfoil without flow control, can be found in [16]. In order to reduce the wall interference effects for this wall-to-wall mounted high-lift configuration, vortex generators have been applied on the upper side of the main wing, as described in [16].

Actuation systems for wind tunnel testing

The actuation systems that are the focus of this publication are presented in figure 3. These are implemented at the model wing leading edge and at the trailing edge flap. Each actuation system consists of a pressure supply, a fast switching valve and an actuation chamber. The shape of these actuation chambers is designed for the specific applications. At the wing leading edge, there is a flow through round inclined holes and the flow control methodology is known as vortex generator jets (VGJs). At the trailing edge flap, the actuator chambers have a rectangular-exit shape that is used for the pulsed blowing flow control method.

The applications with VGJs have a long tradition at TUBS. For two-dimensional models, the optimized actuation has counter-rotating pairs of vortices as used by Scholz et al. in [17], whereas Hühne et al.

[18] reported, for a swept wing application, a co-rotating actuation that was found by numerical research to be more favorable. All studied cases with leading edge control have targeted the delay of the wing stall, with a leading edge-stall type characterizing the baseline configuration. The position of the actuators was of early concern and the best compromise was found to be a lower side actuation at $1\%c$, since the local velocity ratio is higher than for an application on the leading edge upper side. With actuator diameters of the order of $d = 1\text{mm}$, the actuation exit maximum velocities are close to the speed of sound. The application of VGJs allows the formation of strong streamwise vortices that transfer high-momentum close to the airfoil surface and can delay the occurrence of flow separation. The use of the VGJs in a pulsed mode was found to be more energy efficient than continuous blowing.

The trailing edge actuation concerned single and multiple actuation slots for the NWB and KKK tests respectively. The slots are inclined downstream with $\alpha_{\text{jet}} = 30^\circ\text{-}45^\circ$, but not tangential, and have a thin opening of only $w_{\text{jet}} = 0.3\text{mm}$, which was reported by Haucke et al. [19] to be suitable for separation control. This control technique has a long tradition at TUB. The flap flow control systems are designed for actuation intensities with Mach numbers $M < 1$, but higher than the corresponding incoming flow. The actuators are positioned on the flap upper side and ideally close to the separation onset location. Here, the single actuation is at $20\%c$ and an additional $50\%c$ location was taken into account for the multiple-actuation. The length of the actuator-slot is typically infringed by the installation space in the flap. The slotted pulsed blowing actuation allows the formation of spanwise vortices. When the actuation frequency exceeds a specific value, mostly related to the shedding vortices of the baseline flow separation, then the vortices that roll downstream can effectively suppress the separation in a time-average sense. However, vortical structures exist above the actuated surface for every time-instant. Contrary to a tangential continuous blowing, like a Coanda flap, the actuation direction is not efficient for a non-separated baseline flow. The inclined downstream

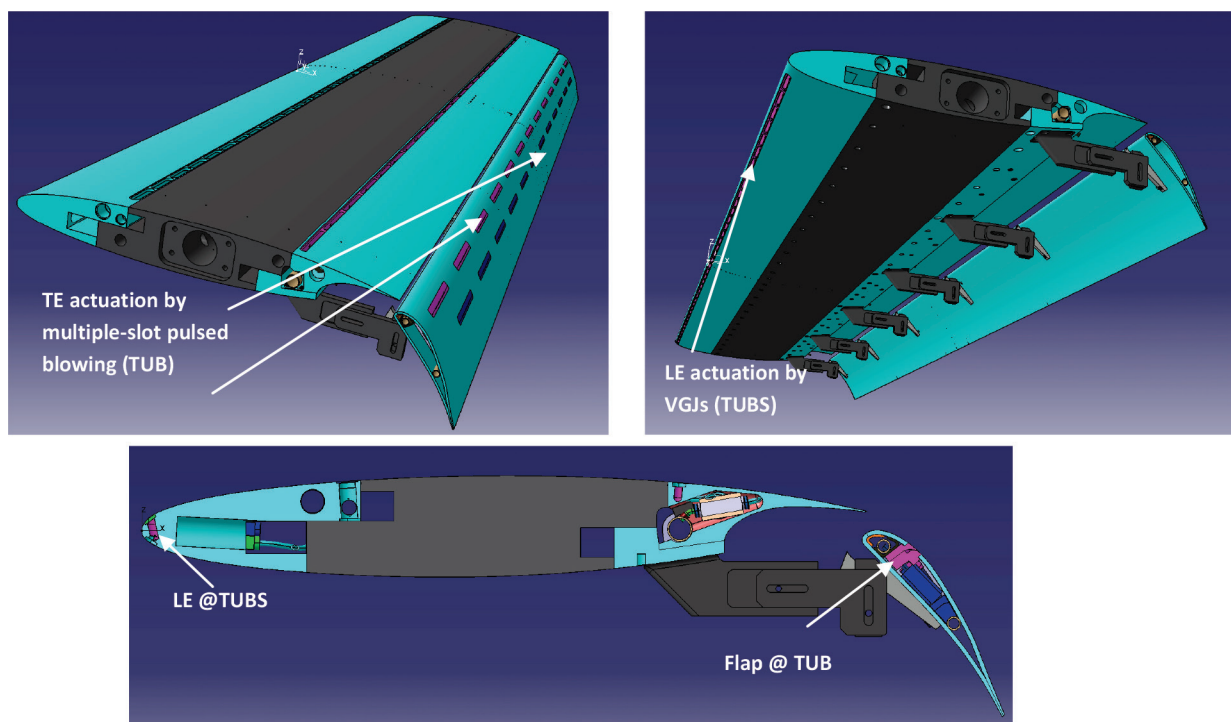


Figure 3 - Actuation systems implemented on the DLR F15 model

actuation velocity vector with $\alpha_{jet} = 30^\circ-45^\circ$ can be divided into two components: a normal and a tangent vector. The first allows for the formation of spanwise vortices that transfer high momentum to the surface during the time-dependent actuation. The latter introduces a thin jet of high-pressure air into the boundary layer to re-energize it, with local velocities higher than those of the outer flow. The resulting velocity vector is favorable for the time-dependent pulsed blowing actuation for separation control.

The parameters used in relation with the active flow control application are the blowing momentum coefficient C_μ , the non-dimensional actuation frequency F^+ and the actuation duty cycle DC. The blowing momentum coefficient was first introduced by Poisson-Quinton [20] and, for this application, is defined as:

$$C_\mu = \frac{\dot{m}_{jet} \times u_{jet}}{\frac{1}{2} \times \rho_\infty \times U_\infty^2 \times A_{ref}} \quad (1)$$

where, in the fraction numerator, \dot{m}_{jet} is the time-averaged actuation mass-flow and u_{jet} is the time-averaged jet velocity. The fraction denominator is the product of the dynamic pressure ($0.5\rho U^2$) and the airfoil reference area, A_{ref} . This variable is a measure of energy consumption. For the active flow control application, a drag coefficient can be associated with the local actuation jet and this is defined, for example, according to Engler [21], as

$$C_D = C_\mu \frac{U_\infty}{u_{jet}} \quad (2)$$

The non-dimensional actuation frequency F^+ is defined as:

$$F^+ = \frac{f \times c_f}{U_\infty} \quad (3)$$

where f is the physical actuation frequency. The characteristic length for determining this variable is the flap chord length c_f and the characteristic velocity is the reference inflow speed.

The actuation duty cycle DC shows the percentage of time in which the actuation valve remains open relative to the actuation period T :

$$DC = \frac{t_{open}}{T} \quad (4)$$

Other characteristics of the actuation components and design specifications can be found in the above mentioned references, e.g. [10]; [18]; [19].

Results

Figure 4 shows the maximum lift increments by separated and combined wing leading edge and trailing edge flap active flow control from the atmospheric wind tunnel testing. The actuation on the wing leading edge mostly shows an increase in the maximum angle of attack, where the flap actuation promotes a shift of the C_L - α -curve. The combined flow control applications show a significant increase in maximum lift, in comparison with the baseline configuration. Each flow control system seems to allow for lift increments of the order of $\Delta C_L \approx 0.15$ and the combined actuation delivers an increase of $\Delta C_L \approx 0.3$ with a $\Delta \alpha_{CL,max} \approx 5^\circ$.

Figure 5 illustrates the maximum lift increments by separated and combined wing leading edge and trailing edge flap active flow control

from the cryogenic wind tunnel testing. Here, a more complex flap flow control setup is in use, namely by multiple-slot actuation. Like for the atmospheric tunnel testing, the wing leading edge mostly shows an increase in the maximum angle of attack where the flap actuation promotes a shift of the C_L - α -curve, now at high Reynolds number. The combined actuation is able to illustrate both enhancements for the maximum lift, as well as for the corresponding maximum angle of attack. The trailing edge actuation shows a lift enhancement of the order of $\Delta C_L \approx 0.6$ in the linear lift regime and $\Delta C_{L,max} \approx 0.4$, whereas the VGJs at wing LE show an increment of $\Delta C_{L,max} \approx 0.1$. The combined actuation indicates a noticeable maximum lift increase and proves the feasibility of the technologies, also at high Reynolds numbers.

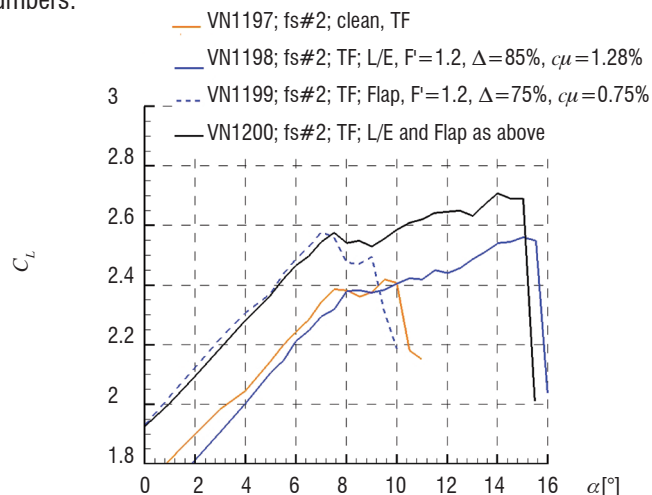


Figure 4 - The maximum lift improvements by vortex generator jets applied at the wing leading edge and single slot pulsed blowing at the trailing edge flap ($M=0.15$, $Re=2 \times 10^6$, $T=290K$, atmospheric wind tunnel testing)

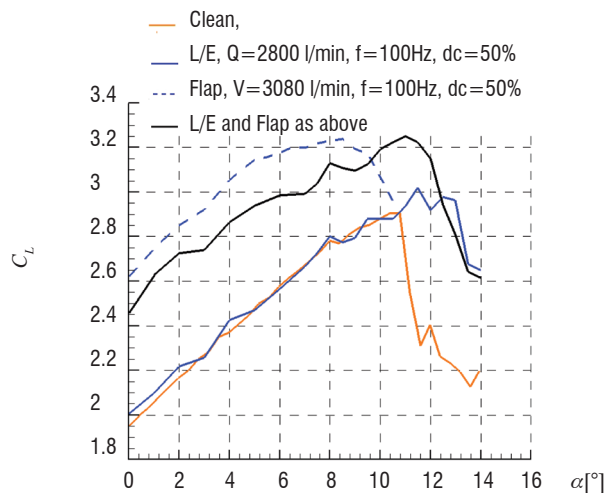


Figure 5 - The maximum lift improvements at high Reynolds number by vortex generator jets applied at the wing leading edge and multi-slot pulsed blowing at the trailing edge flap ($M=0.15$, $Re=4.2 \times 10^6$, $T=170K$, cryogenic wind tunnel testing).

Cryogenic flow control applications have used blowing momentum coefficients of the order of $c_\mu \approx 0.5\%$ for the leading application and $c_\mu \approx 0.15\%$ for the flap actuation, where the frequencies tested are of the order of hundreds of Hertz. Complex cryogenic wind tunnel testing has been very challenging in regard to system implementation, monitoring and results analysis. The reader is advised that individual detailed results concerning the Mach number and Reynolds number variations can be found in the work of Casper et al.[22] and Haucke

and Nitsche [23]. In general, the leading edge flow control shows maximum lift increments up to the flight Reynolds number for moderate mass-flow requirements. Unfortunately, the lift improvement decreases with the increase in Reynolds number and remains below a desired $\Delta C_L \approx 0.5$. Nevertheless, further lift improvements with this actuation system are not excluded. The flap flow control showed a high potential to suppress the local separation with moderate mass-flow requirements at high Reynolds numbers, where tests up to $Re = 7 \times 10^6$ (not shown here) indicate no detrimental impact of the increase in Reynolds number. Moreover, the baseline flow showed an increase in flow separation above the flap, which allows larger overall lift increments by AFC than noticed at low Reynolds.

Flow Control numerical simulations

The numerical results reported in this article concern steady and unsteady Reynolds Averaged Navier-Stokes computations. Research

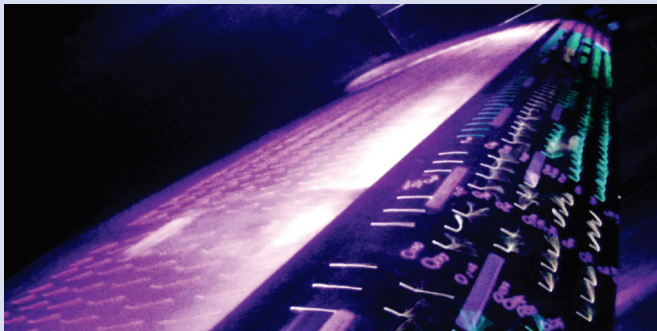
communities worldwide use various RANS solvers for solving different flow control problems, on a large scale. Among these, the reader is advised to consult the published works with the numerical solvers: elsA at Onera, France (e.g. Menuier [25], Dandois [26]), FUN2D at NASA, USA (e.g. Anders [27]), OVERFLOW at Boeing, USA (e.g. Shmilovich [28]), and Edge at KTH, Sweden (e.g. [29]). In the following, the typical DLR TAU solver setups, the mesh generation approach and corresponding results are presented.

The numerical method

The flow solver used is the finite volume compressible solver TAU developed at the German Aerospace Center (DLR) [30]. A second order central scheme is used for the discretization of the convective fluxes. Artificial dissipation is applied, with a 2nd order dissipation term of 1/2 and a 4th order dissipation coefficient of 1/64. The chosen approach for the time integration is either a 3-stage Runge-Kutta time integration method using a CFL number of the order of

Box 1. Active Flow Control on the swept wing high-lift model DLR-F15 in the DNW-NWB wind tunnel

By the end of 2011, wind tunnel investigations have been successfully carried out for the first time with the swept DLR-F15 high-lift airfoil. A unique study to evaluate the capability for aerodynamic enhancement by active flow control (AFC) was addressed within the European program JTI-SFWA [24] at the DNW-NWB facility, in close cooperation with Airbus, TU Berlin and TU Braunschweig. The 2.5D mid-scale test (30° sweep) was performed for a slatless configuration with the most receptive flap setup for AFC; a setup that allowed for the largest lift gains in previous 2D experiments. The results show significant lift enhancements by AFC beyond the optimized clean configuration, especially for moderate angles of attack; the major contributor is the trailing edge AFC application, as indicated by the image. The results confirm previous findings on the 2D wall-to-wall setup of the DLR-F15 and are valuable towards achieving a higher technology readiness level of the AFC technology.



(a) without flow control



(b) with flow control

Figure B1- 01 Tufts visualizations, focusing on the trailing edge flap for the lift enhancement by active flow control



Figure B1- 02 Overview of the mounted swept DLR-F15 model in a DNW-NWB low speed atmospheric tunnel

1.2, or a semi-implicit Lower Upper Gauss-Seidel scheme with a CFL number of the order of 5. In addition to a point explicit residual smoother, convergence is typically accelerated with a 3W-multigrid cycle. For flow control simulations, a transpiration boundary condition that defines the inflow parameters at the actuation surface is implemented.

The grid generation

Perhaps one of the most time-consuming parts of the numerical simulation for high-lift flow control with RANS is the mesh generation. Today, there is no ideal tool for grid generation, but the available software supports the desired mesh topologies that include portions of the slot for a more accurate flow control simulation. The first examples concern applications with the DLR structured-dominant mesh generator MegaCADs [31], [32]. The other computations make use of the hybrid unstructured grid generator, Centaur [33].

For geometries of moderate complexity, a fully structured mesh generation is considered favorable for accurate numerical simulations. However, especially for complex high-lift configurations, or simply with the introduction of slot-actuator portions in the numerical domain, an unstructured approach is more time-efficient. Figure 6 shows the overview for the approach used for round-jet actuators, namely the discretization of the round actuator with quadrilaterals and triangles for the surface vicinity of the VGJ. This approach was successfully verified for single and multiple actuators, including the application of high-lift airfoils. The mesh for the single actuator on a long flat plate has 3 million points and the airfoil mesh contains about 10 million grid nodes. A grid refinement study concluded that the number of structured stacks required for boundary layer flow control is about twice that without control and this is about 60 grid points for the boundary layer discretization. These meshes allow the use of structured cells with large aspect ratio and typically tetrahedrons at the outer domain boundary. Figure 7 shows the second grid generation approach

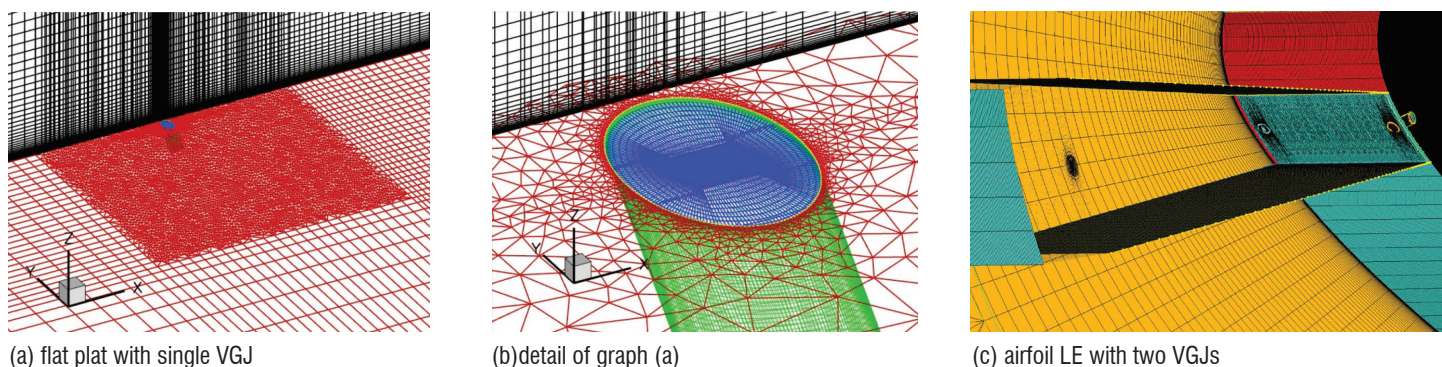
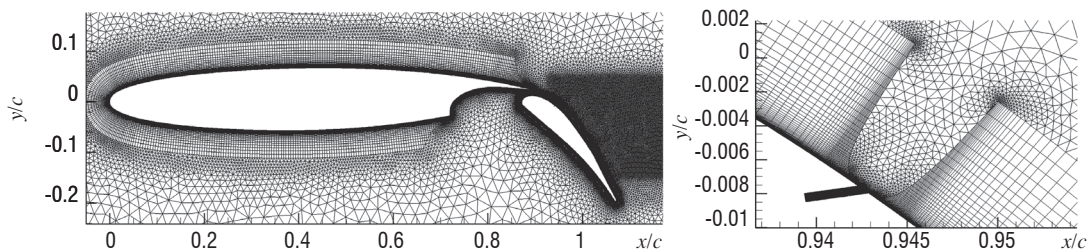
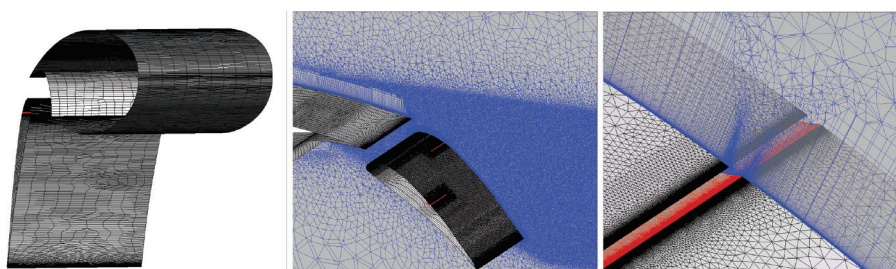


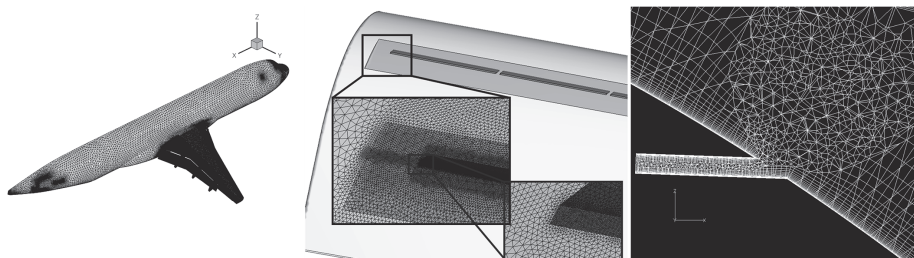
Figure 6 - Overview of the unstructured mesh topology for the round jet simulations, according to [11]



(a) two-dimensional grid for the DLR-F15 airfoil with single-slot-actuator



(b) three-dimensional grid for the DLR-F15 airfoil with two-slot-actuator



(c) three-dimensional grid for a wing-body configuration with 21 slot-actuators

Figure 7 - Overview of unstructured grid topologies for single and multiple slot actuation

frequently used for the flap flow control applications. With the use of the unstructured grid generator, the slits are modeled as a typical pipe with viscous walls. In between the structured stacks, triangular and tetrahedral cells are generated in 2D and 3D respectively. With this approach, grids for single and multiple-actuator have been generated up to a very high level of complexity, namely a wing-body configuration with a trailing edge flap that includes 21 actuators.

Constant blowing VGJs

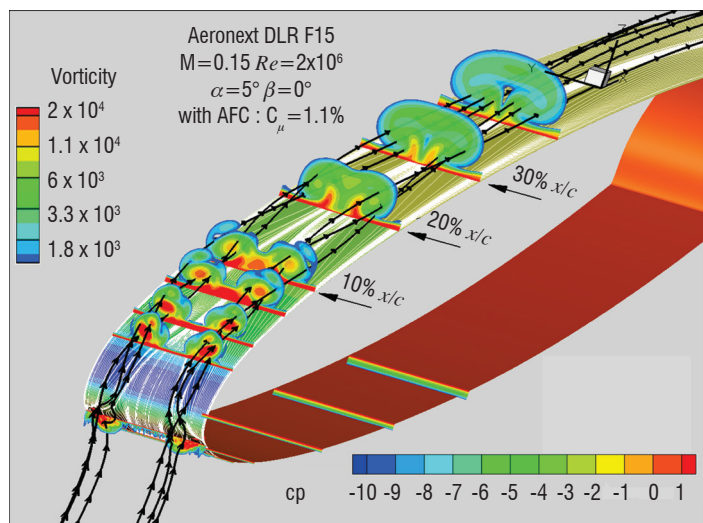


Figure 9 - Numerical simulations with the two-dimensional DLR-F15 airfoil actuated by skewed round jets on the wing leading edge pressure side

A single skewed round jet actuator mounted on a zero-pressure gradient flat plate is the most basic setup used for the verification and validation of the numerical steady RANS method. Constant blowing with an actuation velocity ratio relative to the inflow conditions larger than two promotes a strong streamwise vortex according to experiment and simulation. Figure 8 shows the computed and measured streamwise and normal velocity components in a plane downstream from the actuation. The graphs show the presence of so-called common flow-up and common flow-down, which are responsible for reduction and increase of the velocity magnitude close to the surface. Several state of the art turbulence models have been investigated and Togiti et al. [11] found that the vortex strength and its position are best simulated with a Reynolds Stress Model (SSG/LLR- ω) in comparison with the experiment. However, all models performed fairly well. Figure 9 illustrates the application of this numerical method with a

two-dimensional high-lift airfoil actuated at the wing leading edge by a pair of divergent skewed round jet actuators. Streamwise vortices form on the wing pressure side and remain close to the airfoil surface on the wing suction side after passing the nose region, which is characterized by a very large negative pressure gradient. The vortices are visible over up to more than 30% of the wing chord, where these move closer to each other and become weaker the further the position downstream from the actuators is.

Pulsed blowing slot-actuation

A pulsed blowing application on the flap of a 2-element high-lift airfoil DLR-F15 is sketched in figure 10, for a moderate angle of attack. The single-slot actuation uses a square-shape signal and, over one actuation cycle, the flow above the actuated flap shows the evidence of time-dependent spanwise vortical structures. The time-averaged vorticity distribution shows that a separation persistent in the baseline flow field is reduced in size by active flow control. The aerodynamic lift coefficient is therefore increased as the airfoil circulation increases and the time dependent lift typically shows a periodic oscillation.

With the variation of the blowing momentum coefficient, which is a measure of energy requirements relative to the inflow conditions, the lift increment can be increased or reduced, for example, as required by the targeted flight conditions. Figure 11 illustrates the simulation results for this blowing momentum coefficient effect, where large increments can be obtained by moderate mass flows. However, there is a minimum blowing momentum that must be exceeded in order to obtain a benefit from the actuation. Also, saturation can be reached, which corresponds to an attached flow downstream the actuation.

The comparison of the computed aerodynamic lift coefficients and pressure distributions with the experiment is a matter of the validation process for the numerical method. Figure 12 illustrates the lift coefficients over the angle of attack for the baseline flow and for the best experimentally found actuated setup. The pulsed blowing is an unsteady phenomenon but, as before, the results are time-averaged. Despite particular differences, the aerodynamic behavior observed during the wind tunnel tests could be numerically restituted the lift increments by AFC for the linear lift regime are of the order of $\Delta C_L \approx 0.5$ and the effect on maximum lift is reproduced as well. The increased wing loading promotes a decrease in the measured maximum angle attack by a favorable AFC flap application that is correctly simulated. Figure 13 shows the sectional time-averaged pressure distribution, with and

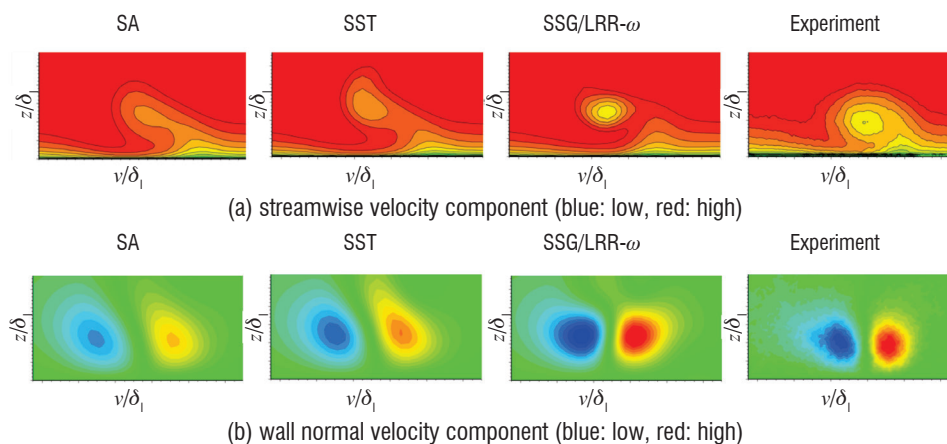


Figure 8 Numerical simulation with two eddy viscosity turbulence models and a Reynolds Stress model for the validation of constant blowing actuation through holes on a zero-pressure gradient flat plate at $2.4 \times \delta_1$ downstream the actuator, according to [11]

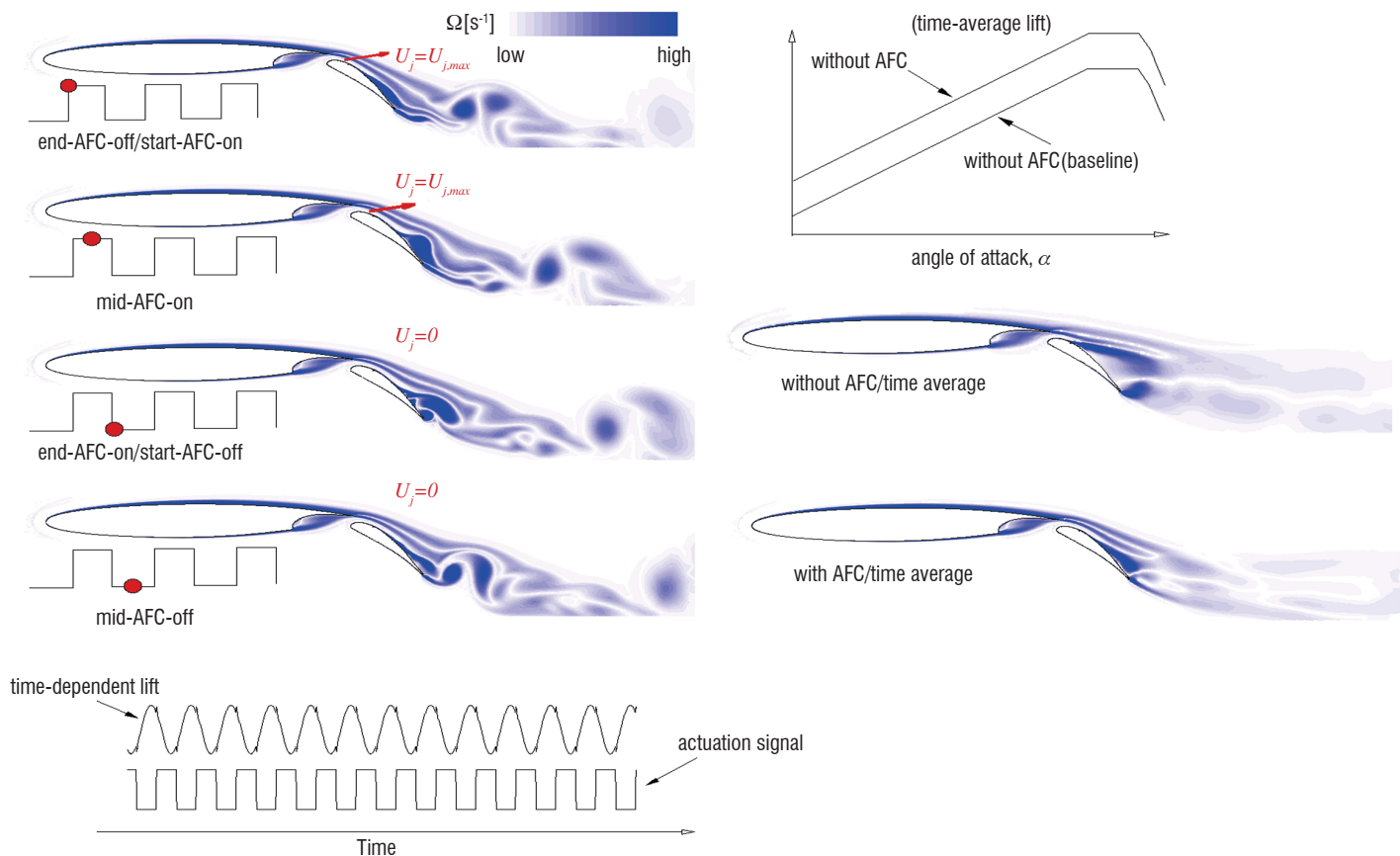


Figure 10 - Schematic view of aerodynamic changes for global and local quantities due to the time-dep pulsed blowing actuation, where the effects over one actuation cycle are shown with computed vorticity flowfields

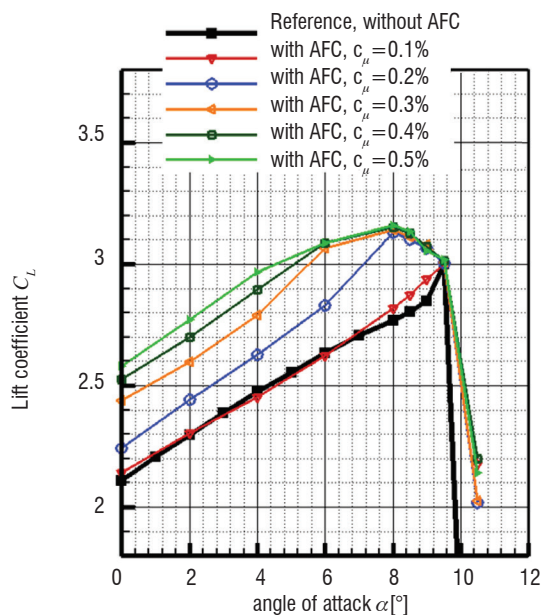


Figure 11 - Lift coefficient over the angle of attack for the DLR-F15 airfoil from URANS simulations, with and without AFC, according to [13]; configuration: 2eOpt49; inflow conditions: $M=0.15$, $Re=2 \times 10^6$

without AFC. The flow separation above the flap is evident in the baseline pressure plateau for the flap upper side, according to the black symbols and lines. This flow separation is considerably reduced as the actuation is switched on and the flap pressure indicates a higher suction peak. The increased flap circulation induces an increase in

the wing trailing edge velocity, with a lower local static pressure and an overall wing circulation enhancement. With the unsteady RANS method, the time-averaged effects are accurately simulated in comparison with the wind tunnel test.

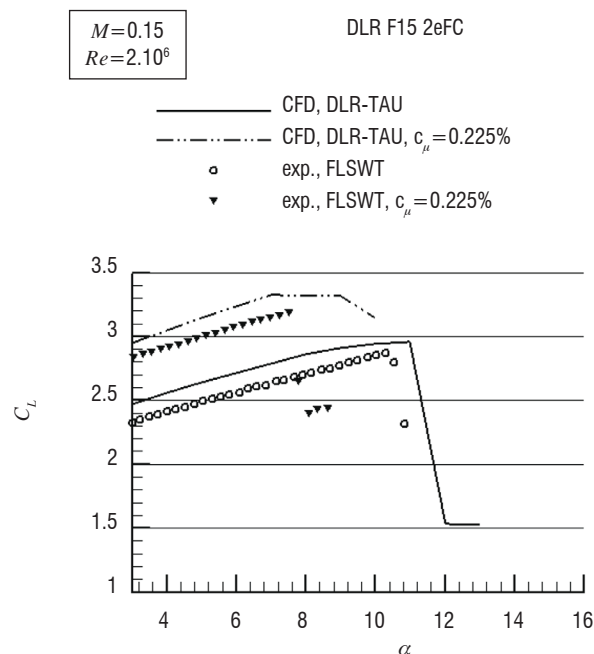


Figure 12 - Computed time-averaged lift over the angle of attack by URANS simulations in comparison with windtunnel measurements for the DLR-F15 airfoil, with and without flow control

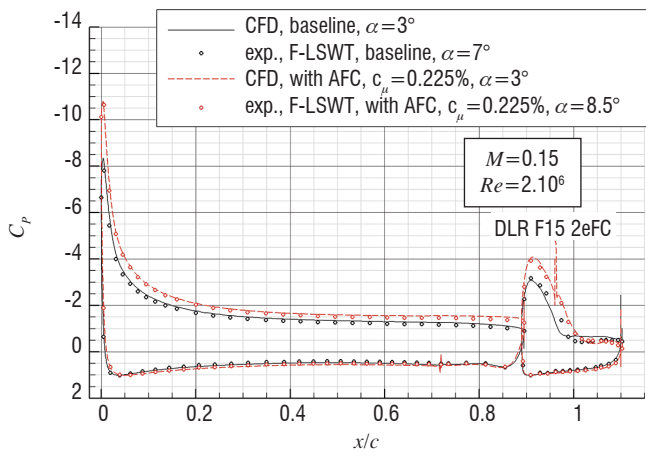


Figure 13 - Computed time-averaged pressure distributions by URANS simulations, in comparison with windtunnel measurements for the DLR-F15 airfoil, with and without flow control; configuration: 2eFC; inflow conditions: $M=0.15$, $Re=2 \times 10^6$

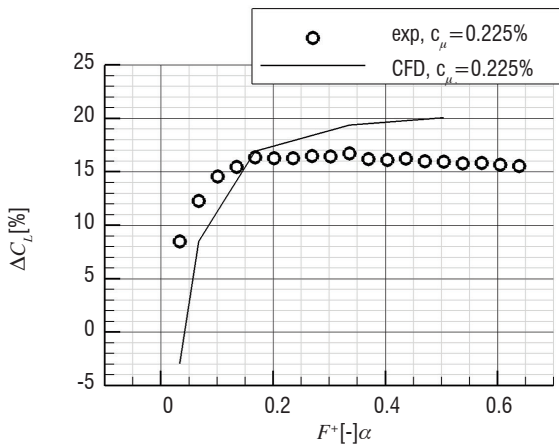


Figure 14 - Computed time-averaged lift over the actuation frequency by URANS simulations, in comparison with windtunnel measurements for the DLR-F15 airfoil with flow control at moderate blowing momentum coefficient; configuration: 2eFC; inflow conditions: $M=0.15$, $Re=2 \times 10^6$

Early wind tunnel tests have shown that an actuation frequency of the order of hundreds of Hertz is sufficient for significant lift improvements. The variation in time of the actuation frequency, between 0...300 Hz, which corresponds to the non-dimensional actuation frequency F^+ , of the order of 0...1, usually points out two major effects that are illustrated in figure 14. At low actuation frequency, the lift increments are low, but increase rapidly with the increase in frequency until $F^+ \approx 0.2$. At higher actuation frequencies, the lift remains mostly independent of this flow control parameter. This particular flow control effect is mostly accurately simulated with the numerical method. In addition, according to the simulations, the shedding frequency of the baseline flow separation above the flap is of about 0.4 (not shown here). These results agree with early experimental findings, for example Seifert et al. [34] and Greenblatt and Wygnanski [2], which reported a successful application for modern flow control at a frequency of the same order as the natural shedding frequency.

The pulsed blowing through slots using a square shape actuation signal was implemented and simulated for a wing body configuration representative to a narrow-body short range aircraft (see figure 15). The scope was to verify the capability of this flow control technology for application on a real aircraft configuration and to validate the numerical method with the experiment [35]. The aim of using AFC was

to suppress the local flap separation for deflection angles at which the flow without control cannot follow the flap contour. Figure 15 shows an overview from the simulations with and without control. The lower side of the image illustrates the complexity of such a simulation, by integrating the slot-actuator and performing the unsteady simulations. The flow topology for the baseline flow is shown in the upper left picture, where on the right side the results are presented for the same inflow conditions but with active flow control. The shaded time-averaged streamwise velocity iso-surfaces located above the flap indicate the size and location of local flow recirculation regions. It is obvious that, from left to right, the flow situation was improved and only sparse local flow separations remain visible, which are actually downstream the non-actuated flap portions. The static surface pressure decreases for wing and flap upper sides with the actuation switched on and this corresponds to an increased lift with about $\Delta C_L \approx 0.4$. Because the used blowing momentum coefficient remains moderate, $c_\mu \approx 0.4\%$, one can notice the success of the application for separation control on a real aircraft configuration. Nevertheless, the fact that there is to date no flight test in preparation for this technology shows that many questions concerning the actuation systems and structural integrity still need to be clarified.

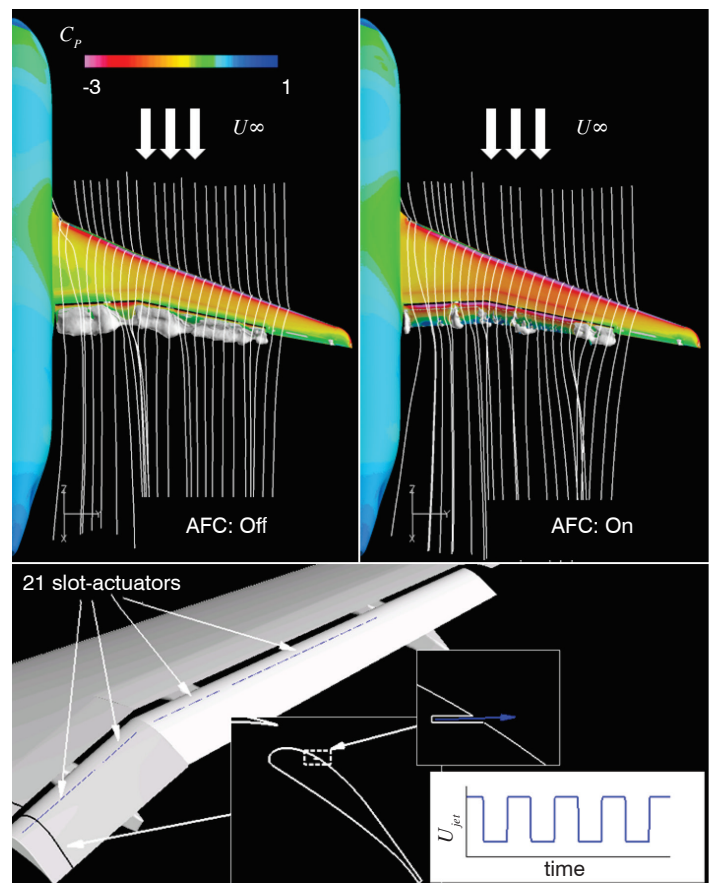


Figure 15 - Overview of numerical results for a high-lift wing body configuration with pulsed blowing separation control

Pulsed blowing through slots proved over the last years to perform well experimentally and numerically. Therefore, there have been questions on how to obtain further improvements. E.g., Hoell et al. [36] were concerned with a distributed actuation in order to find the most appropriate spacing based on CFD for energy efficient actuation. One of the latest reported experimental results in the literature, by Haucke and Nitsche, also concerns multiple and distributed actuation [37]. Nevertheless, an open subject remains for the baseline flow, the configuration that is to be controlled and the past applications have

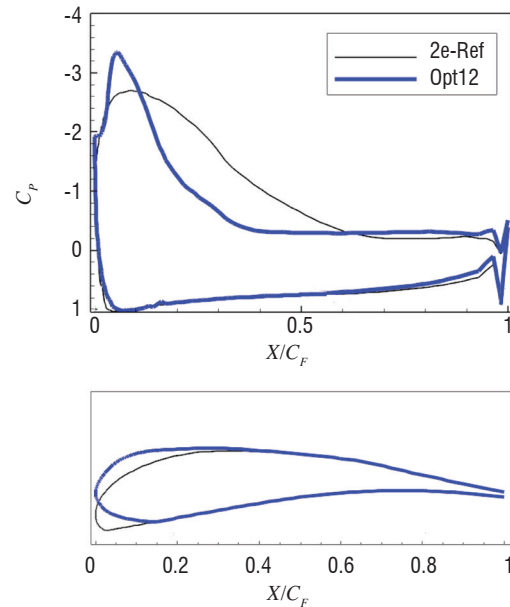
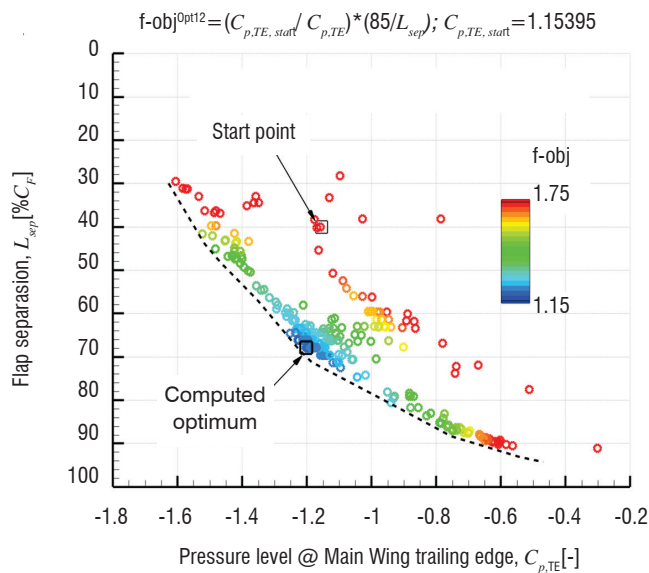


Figure 16 - Results of flap shape optimization for flow control application: pareto-front diagram (left) and corresponding shape and pressure distribution of the baseline flow from start point and optimized shape (right)

been a retrofit flap shape in most of the cases. A higher potential for flow control is expected for a dedicated flap designed for the modern flow control application. Figure 16 illustrates the results of a unique effort to optimize the flap contour through a numerical method, in the search for a better receptivity for the flow control application. The objective for the numerical algorithm was to minimize a function, which corresponds to the increase of flap separation, while decreasing the wing upper trailing edge static pressure. The Pareto front is illustrated in the left-image and it indicates the optimum for a 70% C_F separated flap flow and with a moderately increased flap suction peak. The nose-up movement for the flap with more flattened upper side for this optimized shape can be seen in the right-image. The resulting pressure distributions are plotted in the upper part of this graph. The application of AFC on this flap was consequently studied numerically (not shown). The results revealed that the new flap is more effective than the best found retrofit at low blowing momentum coefficients, but delivers similar lift enhancement at moderate and high actuation intensity. Additionally, the reduced flap deflection of the optimized flap allows for a significant reduction in drag where the lift remains mostly retained, which was not possible with a retrofit shape. Nevertheless, the benefits of this optimized flap shape were proven over the complete airfoil polar. This is considered to be a small example of what could be the future of high-lift system design, taking into account the potential benefits offered by modern flow control.

Conclusions and prospects

This overview highlights some important aspects for high-lift modern flow control that have been recently investigated at DLR. It shows experimental and numerical results for two control technologies, namely pulsed blowing by skewed round jet actuators for leading edge stall delay and by slot-actuators for flap trailing edge separation control. These technologies have matured over the last decade, concerning the evaluation of the aerodynamic performance. Most of the studies concern the implementation, on a state-of-the-art supercritical high-lift airfoil, up to flight relevant inflow conditions. One major objective was to recover the maximum lift loss due to the slat retraction, by using active flow control. It was shown that the combined actuation systems can support significant lift increments at moderate, as well as for high, Reynolds number flows. The numerical method based on the Navier-Stokes equations was validated with wind tunnel experiments and a first complex study of high-lift wing body configuration with flow control was successfully conducted.

The flow control technologies by pulsed blowing showed significant potential for flight relevant separation control. However, further efforts are needed, especially for system design and integration, as well as for the optimization of energetic requirements prior to use on future transport aircraft ■

Acknowledgements

The authors would like to acknowledge the contributions of the Technical Universities of Berlin and Braunschweig for the achievement of these results. Thus, we would like to thank Marcus Casper, Frank Haucke, Philipp Hühne and Peter Scholz for their efforts in performing the common wind tunnel testing at DNW facilities. Moreover, the experimental work and part of the numerical studies have been conducted within the framework of the German national project LuFo IV M-Fly (Luftfahrtforschungsprogramm IV, Multidisziplinäre flugphysikalische Optimierung) and the support of BMWi is acknowledged herewith. Some of the computational work was performed within the scope of European projects and the financial support from the Seventh Framework Programme of the European Community (Clean Sky Joint Technology and AVERT) is also acknowledged.

References

- [1] M. GAD-EL HAK - *Flow Control: Passive, Active, Reactive Flow Management*. Cambridge Univ. Press, New York, 2000.
- [2] D. GREENBLATT, I. WYGNANSKI - *The Control of Flow Separation by Periodic Excitation*. Progress in Aerospace Sciences, Vol. 36, No. 7, pp. 487–545, 2000.
- [3] J.D. MCLEAN, J.D. CROUCH, R.C. STONER, S. SAKURAI, G.E. SEIDEL, W.M. FEIFEL, H.M. RUSH - *Study of the Application of Separation Control by Unsteady Excitation to Civil Transport Aircraft*. NASA Technical Report CR 209338, 1999.
- [4] R. JOSLIN, D. MILLER - *Fundamentals and Applications of Modern Flow Control*. Progress in Astronautics and Aeronautics, Vol. 231, AIAA, Inc., Reston, Virginia, 2009.
- [5] P.K.C. RUDOLPH - *High-Lift Systems on Commercial Subsonic Airliners*. NASA Technical Report CR 4746, 1996.
- [6] F. TINAPP, W. NITSCHKE - *Separation Control on a High-Lift Configuration by Periodic Excitation*. New Results in Numerical and Experimental Fluid Mechanics III, Vol. 77, Springer-Verlag, Heidelberg, 2002.
- [7] R. PETZ, W. NITSCHKE - *Active Separation Control on the Flap of a Two-Dimensional Generic High-Lift Configuration*. Journal of Aircraft, Vol. 44, No. 3, pp. 865–874, 2007.
- [8] R. BECKER, R. KING, R. PETZ, W. NITSCHKE - *Adaptive Closed-Loop Separation Control on a High-Lift Configuration Using Extremum Seeking*. Journal of Aircraft, Vol. 44, No. 3, pp. 865–874, 2007.
- [9] J. ORTMANN, C.J. KÄHLER - *Investigations of Pulsed Actuators for Active Flow Control Using Phased Locked Stereoscopic Particle Image Velocimetry*. Presented at the 12th. Intl. Symposium for Application of Laser Techniques to Fluid Mechanics, Lisbon, Portugal, 12-15 June, 2004.
- [10] P. SCHOLZ, J. ORTMANN, C.J. KÄHLER, R. RADESPIEL - *Leading Edge Separation Control by Means of Pulsed Jet Actuators*. AIAA-Paper 2006-2850, 2006.
- [11] V. TOGITI, V. CIOBACA, B. EISFELD, T. KNOPP - *Numerical Simulation of Steady Blowing Active Flow Control Using a Differential Reynolds Stress Model*. In Proceedings of CEAS/KATnet II Conference on Key Aerodynamics Technologies, Bremen, Germany, 2009.
- [12] V. CIOBACA - *Simulation of Active Flow Control on the Flap of a 2D High-Lift Configuration*. Notes on Numerical Fluid Mechanics and Multidisciplinary Design, Vol. 112, Springer-Verlag, Berlin, pp. 209–216, 2010.
- [13] V. CIOBACA - *Parameter Study for a Slatless 2D High-Lift Airfoil with Active Separation Control using a URANS Approach*. Notes on Numerical Fluid Mechanics and Multidisciplinary Design, Springer-Verlag, Vol. 121, pp. 135-142, Berlin, 2013.
- [14] G. DARGEL, H. HANSEN, J. WILD, T. STREIT, H. ROSEMAN, K. RICHTER - *Aerodynamische Flügelauslegung mit multifunktionalen Steuerflächen*. DGLR, Bonn [Hrsg.]: DGLR Jahrbuch 2002, DGLR-2002-096, Vol. I, pp. 1605, 2002.
- [15] J. WILD, G. WICHMANN, F. HAUCKE, I. PELTZER, P. SCHOLZ - *Large Scale Separation Flow Control Experiments within the German Flow Control Network*. AIAA Paper 2009-530, 2009.
- [16] J. WILD - *Experimental Investigations of Mach- and Reynolds-Number Dependencies of the Stall Behavior of 2-Element and 3-Element High-Lift Wing Sections*. AIAA Paper 2012-108, 2012.
- [17] P. SCHOLZ, C.J. KÄHLER, R. RADESPIEL, J. WILD, G. WICHMANN - *Active Control of Leading-Edge Separation within the German Flow Control Network*. AIAA Paper 2009-0529, 2009.
- [18] C.P. HÜHNE, P. SCHOLZ, R. RADESPIEL, J. WILD, V. CIOBACA - *Active Control of Leading Edge Flow Separation for a Swept High-Lift Airfoil*. In Proceedings of 61 Deutscher Luft- und Raumfahrtkongress, Berlin 10-12 September, 2012.
- [19] F. HAUCKE, M. BAUER, T. GRUND, W. NITSCHKE, B. GÖLLING - *An Active Flow Control Strategy for High-Lift Flaps*. KATnet II. In Proceedings of CEAS/KATnet II Conference on Key Aerodynamics Technologies, Bremen, Germany, 2009.
- [20] P. POISSON-QUINTON - *Recherches théoriques et expérimentales sur le contrôle de couche limite*. 7th Congress of Applied Mechanics, London, September 1948.
- [21] R.J. ENGLER - *Two-Dimensional Subsonic Wind Tunnel Investigations of a Cambered 30 Percent Thick Circulation Control Airfoil*. AD913411 Report, 1972.
- [22] M. CASPER, P. SCHOLZ, R. RADESPIEL, J. WILD, V. CIOBACA - *Separation Control on a High-Lift Airfoil Using Vortex Generator Jets at High Reynolds Numbers*. AIAA Paper 2011-3442, 2011.
- [23] F. HAUCKE, W. NITSCHKE - *Active Separation Control on a 2D High-Lift Wing Section towards High Reynolds Number Application*. To be published at 31st AIAA Applied Aerodynamics Conference, San Diego, CA, 2013.
- [24] Clean Sky European Project, URL, <http://www.cleansky.eu/>
- [25] M. MEUNIER - *Simulation and Optimization of Flow Control Strategies for Novel High-Lift Configurations*. AIAA Journal, 47(5):1145–1157, 2009.
- [26] J. DANDOIS, E. GARNIER, P. SAGAUT - *Unsteady Simulation of a Synthetic Jet in a Crossflow*. AIAA Journal, 44(2):225–238, 2006.
- [27] S.G. ANDERS, W-L. SELLERS III, A.E. WASHBURN - *Active Flow Control Activities at NASA Langley*. AIAA Paper 2004-2623, 2004.
- [28] A. SHMILOVICH, Y. YADLIN - *Flow Control Techniques for Transport Aircraft*. Journal of Aircraft, 49(3):489–502, 2011.
- [29] F. VON STILLFRIED, S. WALLIN, A.V. JOHANSSON - *Vortex-Generator Models for Zero- and Adverse-Pressure-Gradient Flows*. AIAA Journal, 4(50):855-866, 2012.

- [30] T. GERHOLD - *Overview of the Hybrid RANS Code TAU. MEGAFLOW* . Numerical Flow Simulation for Aircraft Design, Vol. 89 of Notes on Numerical Fluid Mechanics and Multidisciplinary Design, Springer, pp. 81-92, 2005.
- [31] O. BRODERSEN, M. HEPERLE, A. RONZHEIMER, C.-C. ROSSOW, B. SCHÖNING - *The Parametric Grid Generation System MegaCads*. In Proceedings of the 5th Intern. Conf. On Numerical Grid Generation in Comp. Field Simulation, National Science Foundation (NSF), pp. 353-362, 1996. <http://www.megacads.dlr.de>.
- [32] J. WILD - *Smooth Mixed Meshes for Acceleration of RANS CFD in Aircraft Analysis and Design*. AIAA Paper 2011-1267, 2011.
- [33] Centaursoft, <https://www.centaursoft.com> (accessed 2012)
- [34] A. SEIFERT, A. DARABI AND I. WYGNANSKI - *Delay of Airfoil Stall by Periodic Excitation*. Journal of Aircraft, 33(4):691–698, 1996.
- [35] V. CIOBACA, T. KÜHN, R. RUDNIK, M. BAUER, B. GÖLLING, W. BREITENSTEIN - *Active Flow Separation Control on a High-Lift Wing-Body Configuration*. Journal of Aircraft, 50(1):56-72,2013.
- [36] T. HOELL, E. WASSEN, F. THIELE - *Numerical Investigation of Spatially Distributed Actuation on a Three-Element High-Lift Configuration*. In R. King, editor, Active Flow Control II - NNFM 108, Notes on Numerical Fluid Mechanics and Multidisciplinary Design, pages 109–123. Springer, 2010.
- [37] F. HAUCKE, W. NITSCHKE - *Active Flow Control on the Flap of a 2D High-Lift Wing Section at $Re=1\cdot 10^6$* . AIAA-Paper 2011-3359, 2011.

Acronyms

AFC	(Active Flow Control)	KKK	(Kryo Kanal Köln) (Cryogenic Windtunnel Cologne)
DLR	(Deutsches Zentrum für Luft- und Raumfahrt) (German Aerospace Center)	ProHMS	(Prozesskette Hochauftrieb mit multifunktionalen Steuerflächen (process chain for high-lift applying multi-functional control surfaces)
DLR F15	(DLR Forschungskonfiguration Nr. 15) (DLR research configuration No. 15)	LE	(Leading Edge)
CFD	(Computational Fluid Dynamics)	TE	(Trailing Edge)
DNW	(Deutsch-Niederländische Windkanäle) (German Dutch Wind Tunnels)	TUB	(Technische Universität Berlin)
NWB	(Niedergeschwindigkeits-Windkanal Braunschweig) (Low Speed Wind Tunnel Braunschweig)	TUBS	(Technische Universität Braunschweig)

AUTHORS



Vlad Ciobaca received his diploma in 2005 from the University Politehnica Bucharest, Faculty of Aerospace Engineering and he has been a PhD candidate (TU Berlin) since 2011. He is a Research Scientist within the DLR Institute of Aerodynamics and Flow Technology, Transport Aircraft Department and High-Lift Group. His field of research is High-Lift Aerodynamics, with a focus on Flow Control, including Mesh Generation, Numerical Simulations and Experimental Aerodynamics, and Wind Tunnel Simulations.



Jochen Wild received his diploma from TH Darmstadt in 1995, and his PhD from TU Braunschweig in 2001 on “Numerical Optimization of High-Lift Airfoils by solution of RANS equations (transl.)”. He is a “High-Lift” Research Scientist and Team Leader within DLR Institute of Aerodynamics and Flow Technology, Transport Aircraft Department. His field of research is High-Lift Aerodynamics, including Numerical Simulation and Design Optimization, Mesh Generation, Experimental Aerodynamics and Flow Control.